International Journal of Nanoelectronics and Materials
Volume 16 (Special Issue) December 2023 [281-296]

The Influence of Sulfate and Iron Reducing Bacteria on Carbon Steel Corrosion in Marine Environments

Rabiahtul Zulkafli[1], Norinsan Kamil Othman[1,*], Najmiddin Yaakob[2] and Azmi Mohammed Nor[3]

[1]Department of Applied Physics, Faculty of Science and Technology, Universiti Kebangsaan Malaysia, 43600, Bangi, Selangor, Malaysia
[2]Industrial Corrosion Research Center, School of Chemical Engineering, College of Engineering, Universiti Teknologi MARA, 40450, Shah Alam, Selangor, Malaysia
[3]PETRONAS Research Sdn Bhd, Lot 3288&3289, Off Jalan Ayer Hitam, 43000, Kajang Selangor, Malaysia

ABSTRACT

The current study highlights the corrosion consequences observed in API 5L X65 carbon steel when exposed to a marine-like environment containing carbon dioxide (CO_2), in the presence of sulfate- reducing bacteria consortium (C-SRB), iron-reducing bacteria consortium (C-IRB), and a combination of both (C-SRB+C-IRB). The corrosion behaviour was assessed through the utilisation of weight loss and surface analysis techniques. The biofilms and corrosion products were characterised using field emission scanning electron microscopy (FESEM) and infinite focus microscope (IFM), respectively. The results obtained from the weight loss technique provided confirmation that in the absence of bacteria, uniform corrosion was the prevailing mechanism in the medium. The uniform corrosion rate was found to be 0.95 mm/year, which was higher than the pit penetration rate of 0.28 mm/year. The combined actions of the C-SRB+C-IRB consortium result in a synergistic impact, leading to a significantly higher rate of pit penetration compared to the individual activities of SRB. Specifically, the pit penetration rate value of 2.13 mm/year is observed, which is notably higher than the uniform corrosion rate of 0.59 mm/year. The utilisation of surface analysis techniques has shown evidence of the existence of sulfur on carbon steel samples that were subjected to exposure from the C-SRB+C-IRB consortium in a CO_2 environment. This sulphur presence is believed to potentially play a role in the development of the iron sulphide (FeS) layer. FeS presence is a contributing factor to the occurrence of pit corrosion due to the SRB metabolite activities. The activities of these metabolites readily dissolve in the medium, hence altering the chemical interface properties of both the metal and the biofilm. For specimens exposed to C-SRB only, the results obtained were almost identical to exposure to the C- SRB+C-IRB consortium. However, the corrosion rate value measured for the C-SRB+C-IRB consortium was higher due to the synergistic effect of the two bacteria. In conclusion, the presence of C-SRB alone and the consortium of C-SRB+C-IRB in a CO_2 environment induces the formation of pitting corrosion. The findings of this study are presumed to contribute a deep understanding of the microbiology-influenced corrosion (MIC) mechanism in CO_2 environments troubling the oil and gas industry. With a better understanding of MIC, new and improved corrosion prevention strategies can be put into action.

Keywords: CO_2 corrosion, microbiology-influenced corrosion, surface morphology

1. INTRODUCTION

Corrosion-induced failures are commonly documented within the oil and gas sector. Oil and gas field environments inherently exhibit corrosive conditions. The environment encompasses a diverse array of dissolved ions that possess the ability to function as corrosive agents, hence leading to a range of corrosion-related issues and detrimental effects within oil field production facilities. The predominant corrosion mechanism observed in the oil and gas sector is attributed

* Corresponding authors: insan@ukm.edu.my

to the existence of carbon dioxide (CO_2) and hydrogen sulphide (H_2S) gases, along with their associated byproducts. This particular corrosion mechanism has been responsible for around 58% of the overall deterioration experienced within the industry [1].

The phenomenon of sweet corrosion arises as a result of the introduction of CO_2 gas into water, leading to the formation of carbonic acid (H_2CO_3) [2]. The rate of corrosion is expected to escalate with the simultaneous increase in CO_2 concentration, system pressure, and temperature. The process of corrosion manifests gradually and in a localised manner, ultimately leading to the formation of pits. In contrast, acid corrosion refers to the phenomenon of metal surface degradation or rust formation occurring within an acidic environment that contains H_2S. Hydrogen sulphide does not exhibit corrosive properties in isolation. However, when water is present, it becomes highly reactive and aggressive [3]. Moreover, empirical evidence suggests that the presence of corrosion results in the development of a cathodic metal sulphide layer on the metal's surface, predominantly consisting of acidic corrosion byproducts. [4]. Typically, the process of acid corrosion results in the development of pitting on the surface of the metal. Furthermore, the presence of H_2S gas can lead to both metal breakdown and the formation of surface fissures due to the pressure exerted by sulphide [5].

Simultaneously, microorganisms, including bacteria, fungus, archaea, and microalgae, have the potential to induce corrosion through direct and indirect mechanisms, contingent upon the interplay between the microorganisms, materials, and electrolytes involved. Microbiologically influenced corrosion (MIC) is a type of corrosion wherein microorganisms exert a substantial influence on the degradation of certain metals and alloys [6]. It has been estimated that MIC constitutes around 20% of the annual corrosion maintenance expense [7]. Several significant incidents related to MIC have been documented in the literature. These include Prudhoe Bay oil spill in 2006, the release of more than 100,000 tonnes of methane due to a well leak in Alison Canyon, and the establishment of a deep sea tsunami early warning system.[8]–[10].

Sulfate-reducing bacteria (SRB) are a type of anaerobic microorganisms that exhibit the ability to thrive and perform metabolic processes without the presence of oxygen. Rather than relying on oxygen, SRB utilise sulphate as a substrate to generate sulphide as a metabolic byproduct. According to previous research, it has been observed that SRB can function as a catalyst in the reduction conversion of sulphate to sulphide [11]. Besides, other findings found that the presence of SRB in irrigation systems can lead to significant metal corrosion [12]. This is attributed to the enzymatic activity of SRB, which facilitates the rapid reduction of sulphate compounds into H2S. In order for the reduction process to take place, three components are necessary: sulphate, free electrons as an external energy source, and water temperature below 65°C [13]. Mild steel, stainless steel, and carbon steel are commonly employed materials within the petroleum industry, which are susceptible to bacterial corrosion. The bacterium SRB has received significant attention in scientific research due to its status as a widely studied microorganism. This bacterium is widely regarded to have a crucial role in the phenomenon known as MIC, as evidenced by numerous studies [14]–[16].

Iron-reducing bacteria (IRB) is a type of facultative anaerobic bacterium that possesses the ability to reduce Fe3+ ions. These ions serve as a terminal electron acceptor in the bacterium's metabolic processes. Respiration in IRB can be accomplished through two distinct mechanisms. The first involves the electron transport chain in anaerobic respiration. Alternatively, IRB can utilise Fe3+ as a "electron sink" to facilitate additional electron transport in anaerobic conditions. This particular process yields a greater amount of energy compared to fermentation. Notably, ions such as nitrate and ferric can serve as terminal electron acceptors, effectively substituting oxygen in Researchers in the field of steel corrosion have shown interest in ferric reducers, which employ ferric ions as terminal electron acceptors during anaerobic respiration [17].

For instance, the bacterium previously known as *Shewanella putrefaciens* has undergone a taxonomic revision and is now referred to as *Shewanella oneidensis* [18], [19]. Organisms capable of surviving in the absence of oxygen employ a metabolic process known as fermentation, wherein organic substances serve as the final electron acceptor.

The augmentation of adenosine triphosphate (ATP) or the accumulation of stored energy generated during the fermentation process can be enhanced by the incorporation of Fe^{3+} ions as a supplementary electron acceptor or "electron sink" in the absence of oxygen [20]. The proliferation of this particular microbe can be enhanced through the introduction of ferric ions into the surrounding medium or environment. This particular iron reducing agent is commonly observed in many soil and environmental contexts.

To date, there remains a dearth of scholarly investigations pertaining to the examination of MIC in pipelines within a CO_2 atmosphere specifically in Malaysia. The current state of research on the local studies pertaining to the impact of steel corrosion resulting from the combined influence of CO_2 in conjunction with SRB and IRB has not been extensively explored. Prior research has indicated that the corrosion products of $FeCO_3$, which are generated on steel surfaces during the process of CO_2 corrosion, have been subject to degradation or impairment caused by SRB. Consequently, the acceleration of steel corrosion is observed in the presence of SRB inside a solution environment that contains CO_2 [2].

The main aim of this research is to examine the influence of market concentration within the oil and gas industry in Malaysia. Metal pipes frequently encounter corrosive conditions, particularly when subjected to the detrimental effects of SRB and IRB. Previuos report posits that the optimal temperature range for the proliferation of SRB lies between 25˚C and 35˚C [21]. The observed area exhibits striking resemblances to the maritime region in Malaysia, as it shares comparable characteristics. Given the prevailing issue of elevated CO_2 gas content within the gas industry in Malaysia, it is imperative to possess a comprehensive understanding of the corrosion mechanisms associated with MIC in the presence of CO_2 gas. This knowledge is crucial for the effective implementation of corrosion control methods aimed at prevention.

2. MATERIAL AND METHODS

Chemical compositions (wt%) of API 5L X65 carbon steel used in this study were, C: 0.16, Si: 0.45, Mn: 1.65, P: 0.020, S: 0.01, V: 0.09, Nb: 0.05 and Ti: 0.06. This steel sample was subjected to mechanical cutting, resulting in dimensions of 10 mm x 20 mm x 2 mm. The process of applying anti-corrosion paint on carbon steel involves coating the entirety of the material, with the exception of a single surface left untreated. Subsequently, the uncoated surface will be subjected to a grinding procedure utilising emery paper ranging from grit 240 to 1200. During each grinding phase, the coupons were subjected to a washing process using distilled water, followed by rinsing with acetone.

The bacterial stock culture utilised in this study was acquired from the Biological Laboratory at the Faculty of Science and Technology, Universiti Kebangsaan Malaysia (UKM). This consortium underwent a process of isolation from the indigenous crude oil reserves situated in the Peninsular of Malaysia. The consortium was cultivated in a VMNI medium as suggested by Zinkevich, which contains (g/L) 0.5 KH_2PO_4, 1.0 NH_4Cl, 4.5 Na_2SO_4, 0.3 $Na_3C_6H_5O_7$, 0.04 $CaCl_{2.6}H_2O$, 0.06 $MgSO_{4.7}H_2O$, 2.0 casamino acid, 2.0 tryptone, 6.0 sodium lactate, 0.1 ascorbic acid, 0.1 thioglycolic acid and 0.5 $Fe_SO4.7H_2O$ [22]. The VMNI medium was made by utilising sea water that has been purified. The produced medium underwent filtration using cellulose acetate membranes with pore sizes of 0.45 μm and subsequently 0.22 μm. Subsequently, the VMNI medium underwent autoclaving at a temperature of 121°C for a duration of 15 minutes. Following this, it was carefully pipetted with 0.1 mL of trace elements and 0.2 mL of vitamins under cool conditions. To obtain a consortium of

sulfate-reducing bacteria (C-SRB) and a consortium of iron-reducing bacteria (C- IRB), two distinct types of single sulfate-reducing bacteria (SRB) and nine distinct types of single iron-reducing bacteria (IRB) were grown. 5 mL of consortium from stock culture was pipetted into 28 mL VMNI medium and grew in an incubator at 30°C for three days. Then, these consortium batches were centrifuged at 3500 rpm for 5 minutes prior to adding test solution.

In order to investigate the impact of corrosion caused by individual bacteria (C-SRB/C-IRB) and a combined consortium of C-SRB+C-IRB in a CO_2 environment, weight loss experiments were carried out under two conditions: one without any bacteria (serving as a control) and the other in the presence of bacteria. Weight loss test was performed in 1 L glass cell. After 14 days of immersion at 30°C, the coupons were withdrawn and cleaned according to ASTM G1-03. Biofilms and corrosion products on carbon steel samples were respectively characterised by field emission scanning electron microscopy (FESEM) and energy dispersive x-ray spectroscopy (EDX), whereas infinite focus microscope (IFM) to identify the maximum pitting depth on the steel surface.

All tests were performed in triplicate samples. The apparatus setup utilised for the weight loss test conducted in the laboratory is depicted in Figure 1. Weight loss test data were obtained by recording initial and final weight readings of carbon steel specimens before and after immersion. The weight change of carbon steel before and after immersion is used to calculate the uniform corrosion rate using the following equation:

$$\text{Corrosion rate } \left(\frac{\text{mm}}{\text{year}}\right) = \frac{87.6 \times \Delta m}{\rho A t} \quad (1)$$

whereas
Δm = weight loss (mg),
ρ = carbon steel density (g/cm3),
A = specimen surface area (cm2) and
t = specimen exposure time (h).

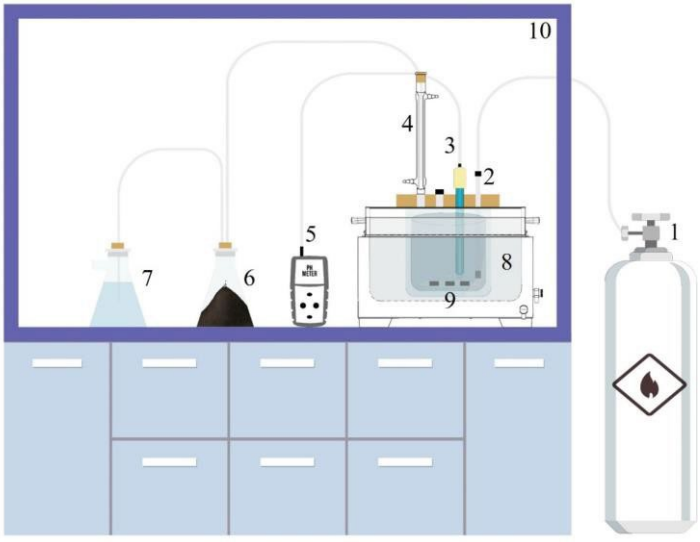

Figure 1. Schematic diagram of the apparatus for the weight loss test 1-CO_2 gas tank; 2-Gas sparger; 3-pH probe; 4-Condenser; 5-pH meter; 6-Activated carbon; 7-Saturated NaOH; 8-Water bath; 9-Carbon steel samples; 10-Fume hood.

The determination of the pit penetration rate is derived from the highest recorded depth of the pitting, as determined through the implementation of the IFM analysis in accordance with the ASTM G 46-94 standard. In order to facilitate the comparison between the uniform corrosion rate and pit penetration rate, this unit will be converted into mm/year by dividing the value by [4]:

$$\frac{Maximum\ depth\ (\mu m)}{Exposure\ time\ (h)} x\ \frac{1\ mm}{1000\ \mu m}\ x\ \frac{24\ h}{1\ day}\ x\ \frac{365\ days}{1\ year} \quad (2)$$

3. RESULTS AND DISCUSSION

The corrosion rate of carbon steel API 5L X65 in a CO_2 environment was assessed using weight loss testing. The experimental conditions involved subjecting the medium to two different scenarios: exposure without bacteria, and exposure with the presence of bacteria (specifically, C-SRB, C-IRB, and a combination of C-SRB and C-IRB). The duration of exposure was set at 14 days, during which a continuous flow of CO_2 was maintained. The determination of the behaviour of corrosion in a given environment can be achieved by analysing various factors such as uniform corrosion rate, pit penetration rate, examination of steel surface microstructure, and the characterisation of corrosion products and biofilm.

3.1 Uniform Corrosion and Pit Penetration Rate

Figure 2 illustrates the comparison between the rates of uniform corrosion and pit penetration for samples of API 5L X65 carbon steel, which were exposed to a CO_2 environment for a duration of 14 days. The corrosion rate value of the control medium during a 14-day exposure period demonstrated the highest value, followed by the combination of C-SRB and C-IRB, C-SRB alone, and C-IRB alone, with corresponding values of 0.95, 0.59, 0.46, and 0.42 mm/year, respectively. Nevertheless, the pit penetration rate exhibited the greatest value of 2.13 mm/year when subjected to C-SRB+C-SRB, surpassing the rates observed in alternative conditions. The sample in C-SRB exhibited the second highest pit penetration rate value among the observed rates for an exposure length of 14 days, measuring 1.40 mm/year. Subsequently, the samples immersed in C-IRB medium and the control yielded pit penetration rate measurements of 0.45 and 0.28 mm/year, respectively.

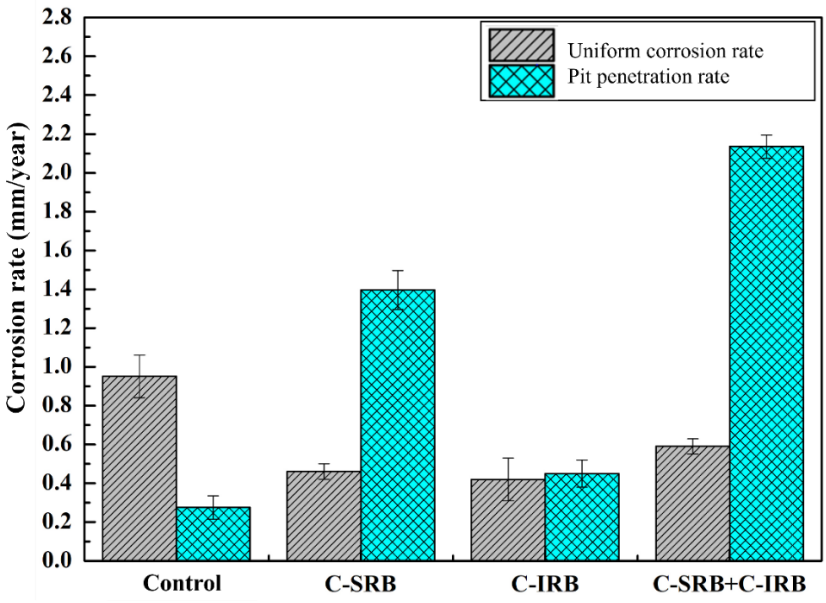

Figure 2. Comparison of uniform corrosion rate and pit penetration rate of carbon steel samples for 14 days exposure time in CO2 environment at 30°C.

The objective of this study was to investigate the role of pitting corrosion in two different environments: a control medium and a medium containing bacteria. The characterization of the pitting factor was conducted to determine the extent of involvement of the pitting corrosion process in these environments. The process of pitting creation is commonly depicted in empirical terms through the utilisation of the pitting factor or pitting ratio. The pitting factor refers to the ratio between the rate at which pits penetrate a material and the rate at which uniform corrosion occurs as stated below:

$$Pittina\ ratio = \frac{Pit\ \ penetration\ \ rate\ \ (mm/year)}{Uniform\ corrosion\ rate\ (mm/year)} \quad (3)$$

The pitting factor was compared between the control medium and the bacterial consortium after a 14-day exposure in a CO_2 environment was shown in Figure 3. The sample exposed to C-SRB+C-IRB exhibited the highest pitting factor value of 3.61, while the sample with the presence of C-SRB had a pitting factor value of 3.04. The values recorded for C-IRB and control medium were 1.07 and 0.29, respectively. A numerical value falling within the range of 2 to 7 signifies the presence of localised corrosion or pitting on the surface [23]. Nevertheless, when the pitting factor is less than 2, it suggests that the steel samples in both the C-IRB and control media are primarily affected by uniform corrosion. This observation demonstrates that carbon steels containing C-SRB and C-SRB+C-IRB exhibit pitting corrosion when exposed to a CO_2 environment for a duration of 14 days, as indicated by the measured values of pit penetration rate.

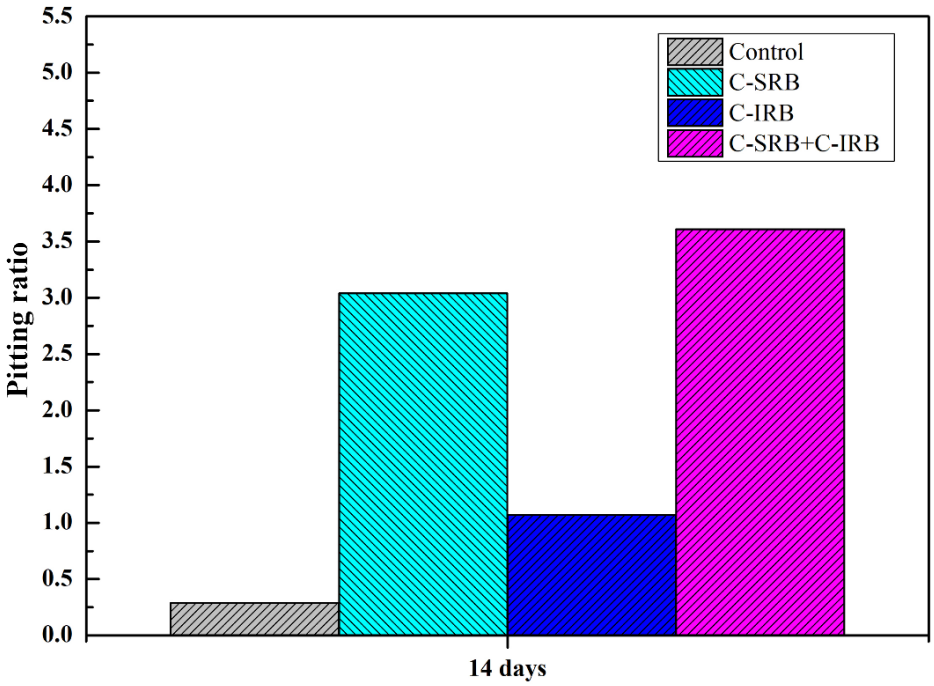

Figure 3. Comparison of pitting ratio factor of API 5L X65 when exposed to control medium, C-SRB, C-IRB and C-SRB+C-IRB for14 days exposure times in CO_2 environment.

3.2 Maximum Pit Depth on Carbon Steel Surfaces

The carbon steel surfaces, which underwent corrosion product removal, were examined in a controlled medium, specifically C-SRB, C-IRB, and C-SRB+C-IRB, under a CO_2 atmosphere for a duration of 14 days. These findings of IFM are depicted in Figure 4. The carbon steel specimen, when subjected to the control media as depicted in Figure 4(a), exhibits a shallow pit with a recorded maximum depth of 10.55 µm. Moreover, the microscope image exhibits a more planar surface. In contrast, Figure 4 (b) illustrates the presence of two significantly deeper pits with exposure of the coupons to C-SRB. The steel surface exhibits a maximum pit depth value of 53.56 µm, which is about five times greater than the control medium's pit depth with the value of 10.55 µm (see Figure 3). A single aperture of 17.25 µm in depth was detected in the carbon steel specimen when immersed in the C-IRB medium, as depicted in Figure 4 (c). This resulted in a pitting ratio of 1.07. Upon exposure to the C-SRB+C-IRB mixture, the coupon exhibits a discernible pit structure, as depicted in Figure 4 (d). The observed pitting structure displays increased width and depth, with a maximum depth of 81.88 µm. The pitting ratio of the sample in the C-SRB+C-IRB medium is reported as 3.61, as shown in Figure 3.

The results indicate that when carbon steel is subjected to medium C-SRB and C-SRB+C-IRB for a duration of 14 days, pitting corrosion occurs. However, in the case of medium control and C-IRB, uniform corrosion remains the predominant form of corrosion observed on the coupons. The carbon steel surface undergoes significant degradation characterised by the formation of a rough structure and the presence of deep, massive pits. This deterioration is attributed to the aggressive environmental attack caused by the production of hydrogen sulphide (H_2S) resulting from the metabolic activities of SRB in both C-SRB and C-SRB+C-IRB media.

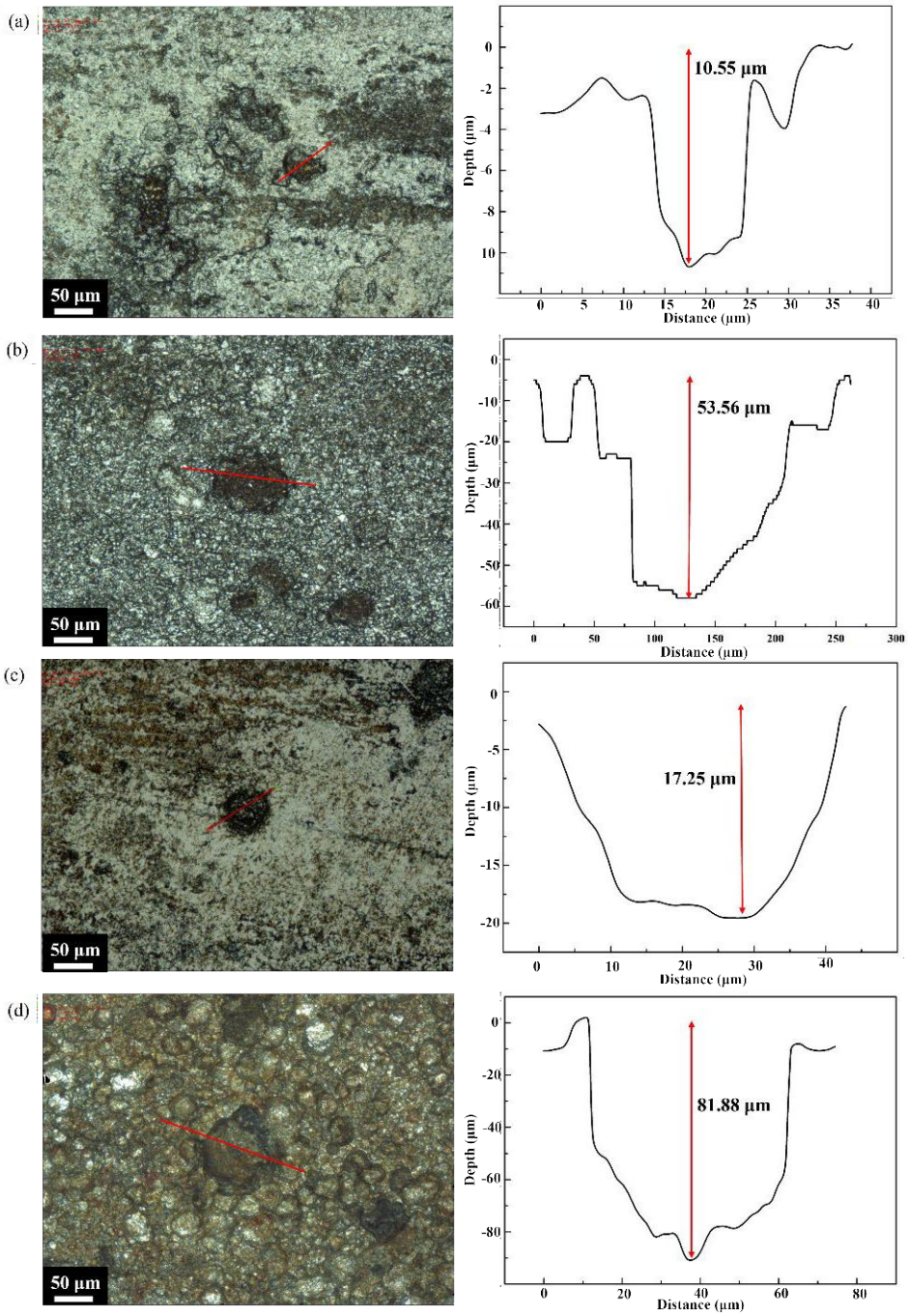

Figure 4. Pit micrographs and maximum depth plots on the surface of carbon steel on medium (a) control, (b) C-SRB, (c) C-IRB and (d) C-SRB+C-IRB in CO_2 environment for 14 days exposure time.

The findings of this study suggest that the inclusion of SRB facilitates the development of more profound pitting on the surface of API 5L X65. The findings given in this study align with previous research on pore depth in CO_2 settings including certain levels of H_2S [24]. The presence of pits observed on surfaces submerged in C-IRB media did not meet the criteria for classifying them as instances of pitting corrosion. This is attributed to the fact that the pitting ratio was found to be less than 2, indicating that the prevailing form of corrosion was predominantly uniform in nature. In contrast, control conditions are characterised by a higher likelihood of the occurrence of uniform corrosion in a CO_2 environment in the absence of H_2S, hence contributing to the overall degradation of the material or metal [25].

3.3 Carbon Steel Microstructure

The morphological analysis of the carbon steel surface exposed to a medium without bacteria and with bacteria, after the removal of the product using FESEM, for a duration of 14 days, is shown in Figure 5. Figure 5 (a and b) depicts micrographs of carbon steel specimens immersed in a control medium observed at magnifications of 2,500X and 5,000X, respectively. One notable observation is the homogeneous occurrence of corrosion on the surface of carbon steel, lacking distinct pitting morphology. The data pertaining to the pitting component (Figure 2 and Figure 3) provide evidence suggesting that samples exposed to a bacteria-free environment have a tendency towards uniform corrosion formation. The surface roughness seen on the steel surface depicted in Figure 5 (a and b) demonstrates that the weight loss occurred uniformly for the sample exposed in the control medium. This finding further reinforces the fact that uniform corrosion has occurred when the steel is exposed to a medium without bacteria.

The presence of a solitary C-SRB consortium bacterium, as presented in Figure 5 (c), is associated with evident pit development. The image depicted in Figure 5 (d) exhibits magnification, revealing the presence of a solitary pits of approximately 2 μm in size. Additionally, two pits that are in close proximity to each other can be detected, as well as two smaller individual pits. These observations were made when the carbon steel was subjected to the C-SRB mixed bacterial consortium system.

The exposure to the C-IRB consortium results in a more uniform roughness, with no visible pits, as shown in Figure 5 (e and f). Additionally, this observation demonstrates that the corrosion occurring is uniform in nature, as opposed to pitting corrosion. In contrast, Figure 5 (g and h) displays a micrograph depicting the surface morphology of carbon steel following exposure to C-SRB+C-IRB, subsequent to the removal of the product, over a period of 14 days. The creation of a deep pit with a rougher surrounding surface is readily apparent.

3.4 Biofilms and Corrosion Product Analysis

The API 5L X65 carbon steel sample was subjected to exposure for a duration of 14 days, resulting in the acquisition of a FESEM image and EDX analysis, as depicted in Figure 6. In accordance with Figure 6 (a), it can be observed that a compact layer is formed. Furthermore, the presence of flower petals was found to be associated with the formation of cracks in the oxide film. The EDX examination (Figure 6 (b)) revealed that the primary elements detected were iron (Fe), oxygen (O), and carbon (C), which are hypothesised to have a role in the development of the corrosion product layer. Additional components that were detected include nitrogen (N), sodium (Na), and chlorine (Cl), which are presumably derived from the VMNI mixture employed as a study substrate. The corrosion product formed as a result of exposure to the control medium is ferric oxide, either FeOOH and Fe_3O_4 which was also confirmed by previous studies through the form of a petaled flower [26], [27].

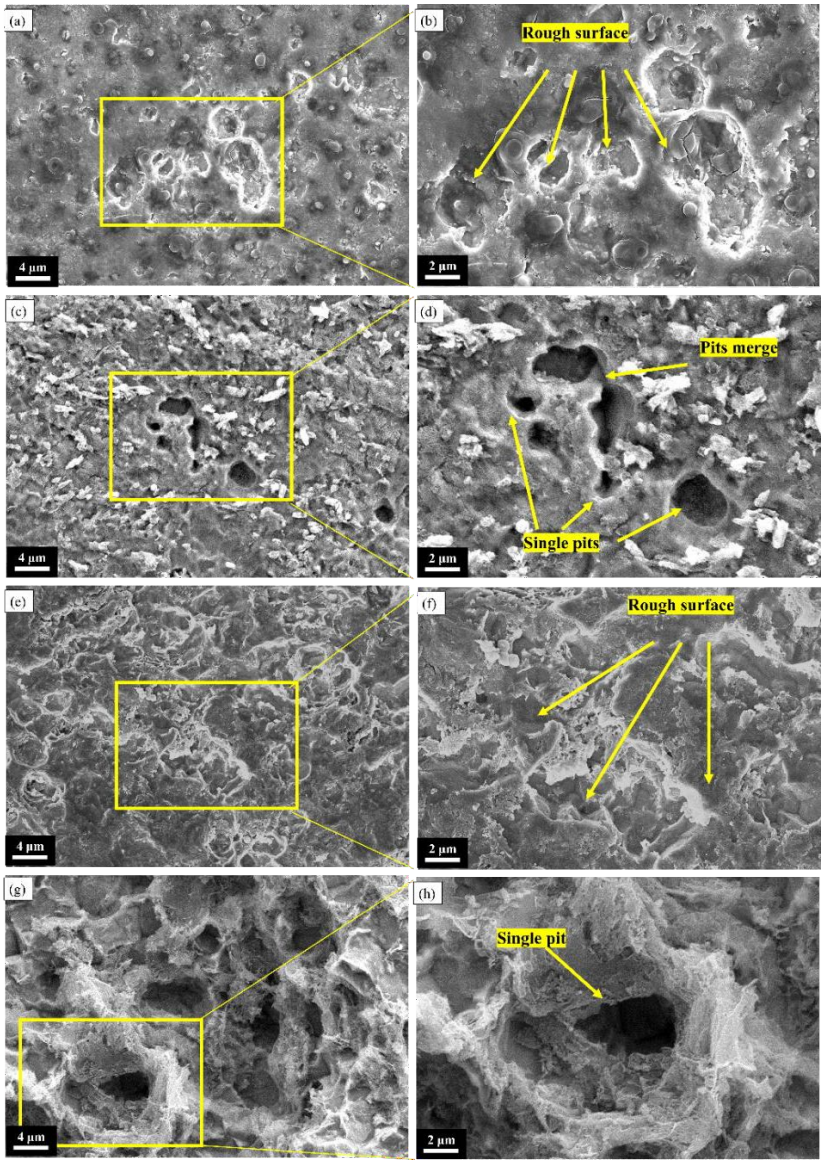

Figure 5. Micrographs of surface morphology of carbon steel over time for 14 days exposure to (a) control medium at 2,500X and (b) 5,000X magnification; (c) C-SRB at 2,500X and (d) 5,000X magnification; (e) C-IRB with 2,500X and (f) 5,000X magnification; (g) C-SRB+C-IRB with 2,500X magnification and (h) 5,000X after removal of corrosion products.

The image depicted in Figure 6 (c) illustrates the visual representation of carbon steel when exposed to C-SRB media. The image clearly demonstrates the creation of cells, which are observed to be densely clustered together and exhibiting an upward growth pattern in a cross-linked way. SRB1 bacterial cells were identified by their spherical shape referring to *Desulfococcy multivorans* species [28]. Meanwhile, the species *Desulfovibrio sp.* belonging to SRB2 was observed with the shape of vibrio or curve with a diameter of 1.5–2.0 µm [29]. Biofilms in SRB are composed of microbial cells, filamentous extracellular polymeric substances (EPS), and metabolic byproducts. These biofilms have been seen to impede the formation of a dense iron sulphide layer, leading to the presence of less compact sulphide precipitates on the surface [11]. The black region is suggested to represent a zone devoid of biofilm growth. The image exhibits a distinct manifestation of EPS encapsulation around SRB cells, displaying uniform growth across the entirety of the carbon steel surface.

The elemental analysis conducted using EDX as shown in Figure 6 (d) reveals that the biofilm mostly consists of Fe, C, O, and sulphur (S). This finding suggests that iron sulphide serves as a metabolite produced by SRB bacteria, in addition to the generation of organic compound corrosion products. Element O is hypothesised to be derived from ferric oxide generated by the oxidation of sulphide when a limited amount of oxygen infiltrates the anaerobic cell's glass [30]. The coexistence of SRB and the synthesis of extracellular polymeric substances (EPS) lead to the diminishment of sulphate and other sulfur-based compounds, such as thiosulfate and sulfite, into sulphide ions, which subsequently induce corrosion [14]. Figure 6 (e) depicts the attributes and qualities of the interface that is encompassed by a heterogeneous layer formed as a consequence of the amalgamation of biofilms and corrosion products. The direct attachment of IRB cell bacteria to metal surfaces is confirmed by micrographs, which demonstrate the accumulation of both round and long rod-shaped bacterial cells. The presence of membrane cells belonging to the C-IRB consortium was seen on the carbon steel surface.

These cells were identified based on their rod-shaped morphology, with lengths ranging from 2.0 to 3.0 µm (S12), 2.0 to 4.0 µm (S17C), and 2.0 to 2.5 µm (S1R) [31]. Additionally, several cells exhibited a rod-shaped morphology like that of cauliflower (S18W) [32]. The examination of the image also found the evident that there are EPS cells, spores, and fibres intermingled on the surface of the coupon. According to Al Abbas *et al*., the biofilm is predominantly covered by EPS and corrosion products, accounting for 75-95% of the total biofilm. The remaining 5-25% is occupied by metabolic cells [33].

The primary elements identified in the analysis Figure 6 (f) are Fe, O and C, indicating the presence of corrosion products formed from the interaction of carbon steel, VMNI medium, and a CO_2 atmosphere. However, a recently found element has been identified as element S. Based on prior research, it has been established that *Shewanella* species is a bacterium that exhibits the ability to do sulphate reduction [34]. This observation was further corroborated by the visual examination of the solution subsequent to the experiment, which exhibited a darkened appearance in the lower region of the cell glass Although *Shewanella* is classified as a sulfate-reducing bacterium, its inclusion in the category of iron-reducing bacteria has rendered its sulfate-reducing activity insignificant in terms of corrosion activity. Previous report posited that the presence of the element S was seen at levels below 1% [35]. Conversely, the present study observed the presence of the element S at a maximum concentration of 3%. The presence of sulphate compounds in the VMNI medium, which serves as an enrichment medium for SRB and IRB, may also contribute to the presence of this S element.

The micrograph depicted in Figure 6 (g) illustrates the effects of exposure to immersion time for up to 14 days in the mixed consortium (C-SRB+C-IRB). The biofilms that formed on the surface exhibited a cohesive structure and demonstrated increased thickness compared to those observed on C-SRB and C-IRB alone The reliability of the cell's shape is diminished due to the presence of EPS corrosion products on its surface. Images provides a clearer depiction of the extracellular polymeric substance (EPS) structure, which encompasses the cell membrane and extends over a significant portion of the carbon steel surface. The biofilm's chemical composition on EDX analysis Figure 6 (h) reveals that its primary constituents are Fe, C, O, and S, with secondary components including N and Cl observed on day 14. Additionally, N, Na, Cl, and manganese (Mn) were detected on day 14. The identification of the primary composition indicates that iron sulphide is among the metabolites produced by microorganisms known as SRB, in addition to the generation of corrosion products derived from organic compounds. The coexistence of SRB and the generation of EPS lead to the conversion of sulphate and other sulfur-based compounds, such as thiosulfate and sulfite, into sulphide ions, which subsequently induce corrosion. Element O is hypothesised to be derived from ferric oxide, which is formed as a result of the oxidation of sulphide in the presence of a limited amount of oxygen that infiltrates the anaerobic cells' glass.

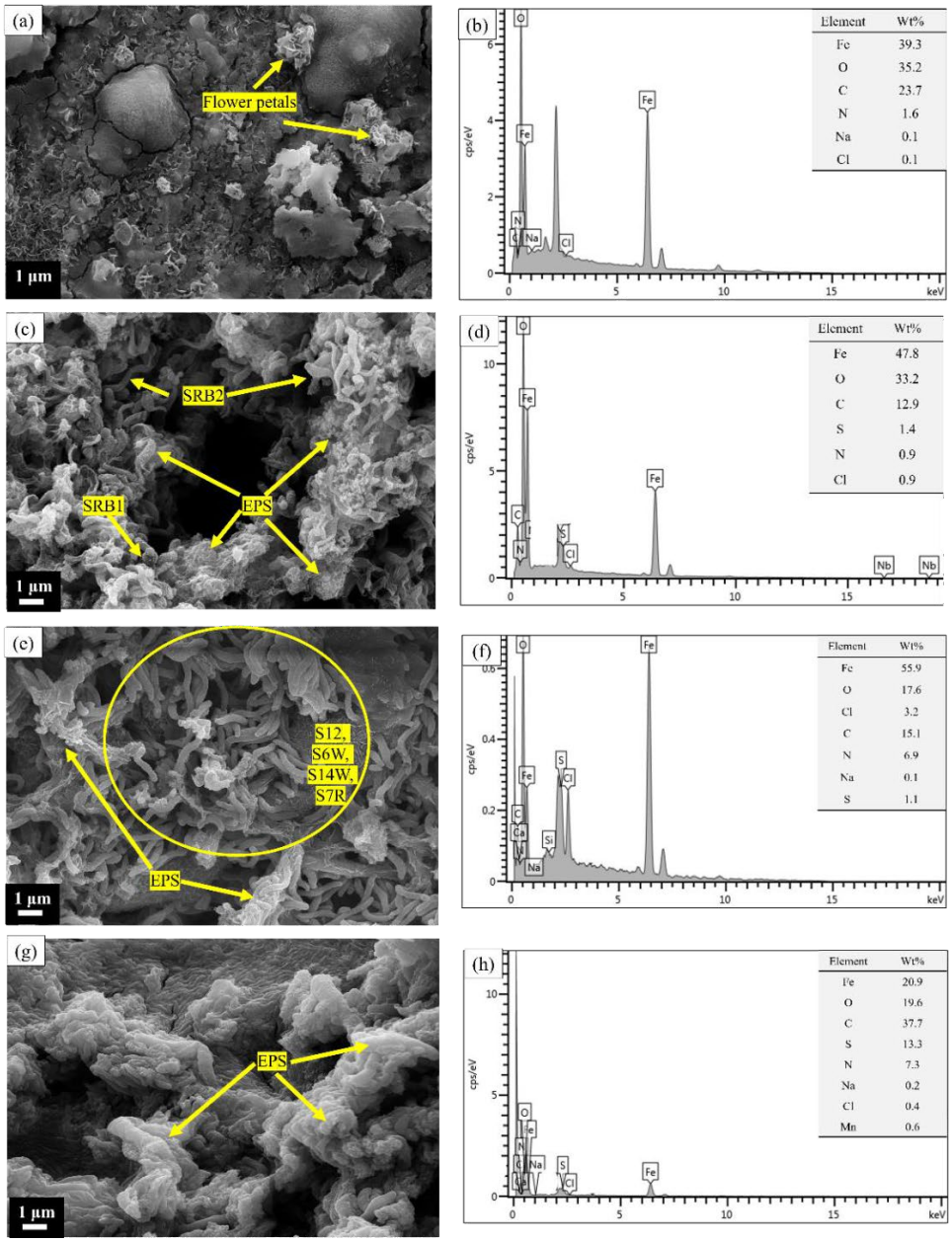

Figure 6. FESEM analysis of carbon steel over time for 14 days exposure to (a) FESEM images and (b) EDX analysis of control medium; (c) FESEM images and (d) EDX analysis of C-SRB; (e) FESEM images and (f) EDX analysis of C-IRB; and (g) FESEM images and (h) EDX analysis of C-SRB+C-IRB.

The process of MIC is initiated when carbon steel surfaces are colonised by C-SRB, leading to the creation of biofilms. Biofilms consist of bacterial cells, EPS, and corrosion products. The biofilm composition is typically comprised of EPS and corrosion products, which account for 75-95% of the total biofilm [36]. Bacterial cells, on the other hand, constitute 5-25% of the biofilm. Bacterial EPS primarily consist of polysaccharides, proteins, nucleic acids, and phospholipids [37]. EPS facilitate bacterial adhesion to metallic surfaces and are believed to have a significant impact on the corrosion phenomenon due to their ability to sequester metal ions, resulting in the formation of highly concentrated cellular structures. Consequently, the production of heterogeneous biofilms characterised by a substantial cell concentration leads to the prevention of corrosion products from being generated within the same localised region. This reaction leads to an increased susceptibility of the metal to localised corrosion, resulting in the development of pitting corrosion.

3.5 The Influence of Bacteria on Carbon Steel Corrosion

The coexistence of bacteria in the CO_2 environment, whether individually as C-SRB or C-IRB, or in a combined state C-SRB+C-IRB, demonstrates that the corrosion rate values remain consistent and do not exhibit substantial variations between these three circumstances. The inclusion of bacteria in C-SRB, C-IRB, and C-SRB+C-IRB has been observed to significantly reduce the uniform corrosion rate of carbon steel, as shown in Figure 2. Specifically, the reduction is around 50% compared to the uniform corrosion rate observed in the control medium. The presence of bacteria in the CO_2 corrosion system leads to the formation of protective corrosion products. The EDX analysis of the corrosion products, namely FeS demonstrates their role in safeguarding the metal against electron loss. This protective mechanism significantly reduces the rate of uniform corrosion when compared to the control medium devoid of bacteria.

In the control medium, which refers to a medium without bacteria, the corrosion products generated were analysed using EDX suggesting the presence of FeOOH and Fe_3O_4 due to the shape of petal flower. The corrosion products that are generated within this CO2 environment devoid of bacteria exhibit features that do not offer protection against corrosion. According to literatures, FeOOH and Fe_3O_4 are categorised as corrosion products that are non-protective and exhibit instability in terms of their potential to provide stability and protection against corrosion [38], [39]. The occurrence of homogenous corrosion attack on carbon steel is attributed to the development of non-protective and unstable corrosion products on its surface. This discovery demonstrates that the level of safeguarding carbon steel surfaces from corrosion is contingent upon the corrosion products that are formed.

The second observation pertains to the impact of the combination of the C-SRB+C-IRB consortium on the pitting ratio, resulting in a twofold augmentation in comparison to the singular C-SRB consortium. In contrast, the pitting ratio of C-SRB exhibited a twofold increase in comparison to C-IRB. Pitting corrosion is initiated through localised fragmentation, resulting in the subsequent formation of pits. The impact of bacteria is significantly affected by the development of biofilms [40]. The attachment of biofilm on steel surfaces exhibits heterogeneity in its strength and does not provide effective protection for the underlying surface. In essence, a rise in the quantity of bacterial cells leads to a corresponding augmentation in the biofilm formation on the surface of carbon steel.

3.6 The Effect of Biofilm on The Formation of Pitting Corrosion

The formation of corrosion pits seen in this study, in the presence of bacteria (namely C-SRB and C-SRB+C-IRB), can be attributed to the presence of sessile cells within the biofilm that is connected to the surface of the metal. According to Jefferson, the primary factors that contribute to the creation of biofilms are the availability of nutrition sources, effective adhesion mechanisms that facilitate the maintenance of an ideal environment, the provision of protection from adverse environmental circumstances, and the potential for mutualistic interactions with other species [41]. When carbon steel is subjected to immersion or exposure in a test environment consisting of VMNI medium with CO_2, the process of organic and non-inorganic molecule attachment takes place within a relatively short period of time, often a few hours.

Subsequently, the formation of a biofilm occurs within a few days following the immersion. It is noteworthy that the testing procedure is conducted alone on the 14th day. The formation of the biofilm is comprised of bacteria, diatoms, and microorganisms embedded within an extracellular polymer substance [42]. The degree of adhesion is contingent upon the characteristics of the substrate, specifically its surface roughness and surface energy, which influence the development of the biofilm [34], [43]. The process of corrosion may initiate during the initial phases of biofilm development.

After their formation, biofilms possess the capability to induce localised modifications in the concentration of dissolved oxygen, chloride, and other ionic species, as well as pH levels. These alterations have a direct impact on the corrosion rate, as observed by Amendola & Acharjee [44]. While the bacteria themselves do not possess corrosive properties, the existence of a biofilm impedes the transport of chemical species through them, potentially resulting in the development of cells exhibiting varying levels of oxygen concentration. The process of oxygen diffusion is observed to exhibit enhanced rates within biofilms that possess perforations or conduits around the microcolonies. The specific region under consideration is probable to be an area devoid of a protective corrosion coating. Consequently, the anaerobic zone beneath the colony is transformed into the anode, while the surrounding solution environment is converted into the cathode [45]. Variations in cellular oxygen concentration may arise when the biofilm selectively adheres to specific regions of the metallic substrate. Nevertheless, some studies have demonstrated that the presence of biofilms composed of non-corrosive bacteria can effectively mitigate corrosion rates through the formation of a protective absorption barrier layer [46]. The aforementioned mechanism has a role in decreasing the corrosion rate of carbon steel samples when they are submerged in a C-IRB solution.

A biofilm has the potential to be comprised only of a single species. The process of biofilm development was observed to include a singular species in both the C-SRB consortium and the C-IRB consortium. Nevertheless, it is worth noting that the majority of biofilms inherently consist of a diverse range of species that come together as consortia, hence exacerbating the corrosion issues they cause [47]. The presence of a greater number of biofilm-forming species in the mixed consortium of C-SRB+C-IRB also had an impact on the augmentation of the pore penetration rate and led to an elevation in pore depth, in contrast to the sole presence of C-SRB. This work examines the capability of C-IRB to reduce Fe^{3+} through its respiration, resulting in the use of Fe^{3+} as a supplementary "electron sink" for electron transport in anaerobic conditions, thus leading to enhanced energy production. The increased energy serves as a carbon source for SRB, hence facilitating the development of biofilms and substantially augmenting the rate of pore penetration. According to Meyer, prior research has indicated that the combination of two aerobic acid-producing bacteria and SRB has the potential to enhance the penetration rate [48].

4. CONCLUSION

The production of uniform corrosion predominates in the solution devoid of microorganisms. In contrast, it is seen that the inclusion of bacteria in the CO_2 environment, whether individually as C-SRB or C-IRB, or in combination as C-SRB+C-IRB, does not result in a substantial alteration in the corrosion rate value across these three situations. The inclusion of bacteria in C-SRB, C-IRB, and C-SRB+C-IRB has been observed to significantly reduce the uniform corrosion rate of carbon steel. Specifically, the reduction is around 50% compared to the uniform corrosion rate observed in the control medium. The occurrence of a solitary consortium consisting of C-SRB and a mixed consortium comprising both C-SRB and C-IRB led to the development of pore corrosion. Specifically, the consortium of C-SRB+C-IRB exhibited a twofold elevation in the pitting ratio compared to the singular consortium of C-SRB.

The characterization of biofilms revealed the presence of well-defined cell membrane structures in samples that were subjected to a bacterial media. The synthesis of EPS can also be noticed as it envelops the cell membrane. The surface of the C-SRB+C-IRB medium has the greatest biofilm density or thickness, whereas the C-SRB and C-IRB media have lower levels. The EDX revealed the mixture of FeOOH and Fe_3O_4 in the control medium. The experimental results demonstrated that when exposed to C-SRB and C-SRB+C-IRB media, the corrosion products formed were FeS. The occurrence of C-SRB and C-SRB+C-IRB had an impact on the development of pitting corrosion. Specifically, the C-SRB+C-IRB consortium exhibited a pitting ratio value that was twice as high as that of the C-SRB consortium alone.

The presence of pits can be attributed to the non-uniform generation of a biofilm layer on the surface of steel, leading to the prevention of corrosion products from forming in a localised region. Consequently, the aforementioned reaction results in the exposure of the metal to a localised corrosion attack, leading to the development of pitting corrosion. The pitting ratio value obtained from the combination of C-SRB and C-IRB is higher compared to that of the solo C-SRB consortium due to its higher cell density.

ACKNOWLEDGEMENTS

We are grateful for the financial support of the Ministry of Education Malaysia (FRGS/1/2020/TK0/UKM/02/35). We thank DNVGL@UKM lab for their experimental facilities to conduct this research project and the Centre of Research and Instrumentation Management (i-CRIM), Universiti Kebangsaan Malaysia for FESEM, EDS and IFM testing.

REFERENCES

[1] Zeng, D., Dong, B., Zeng, F., Yu, Z., Zeng, W., Guo, Y., Peng, Z., Tao, Y., J. Nat. Gas Sci. Eng. vol. 86, issue 7 (2021) pp.103734-103744.
[2] Liu, H., Cheng, Y.F., Corros. Sci., vol. 133, issue 4 (2018) pp. 178–189.
[3] Feng, R., Beck, J. R., Hall, D. M., Buyuksagis, A., Ziomek-Moroz, M., Lvov., S. N., Corrosion, vol. 74, issue 3 (2018) pp. 276–287.
[4] Shah, M., Ayob, M. T. M., Yaakob, N., Embong, Z., Othman, N. K., Corros. Eng. Sci. Technol. vol. 57, issue 1 (2021) pp. 1–17.
[5] Asrar, N., Stipanicev, O. B. M., Jackson, J. E., Jenksin, A., Melot, D., Scheie, J., Vittanato, J., Oilf. Rev., vol. 28, issue 2 (2016) pp. 34–49.
[6] Petrovic, Z., Vojnoteh. Glas., vol. 64, issue 4 (2016) pp. 1048–1064.
[7] Knisz, J., Eckert, R., Gieg, J., FEMS Microbiol. Rev., vol. 47, issue 5 (2023) pp. 1-10.
[8] Conley, S., Franco, G., Faloona,, I. Blake, D.R., Peischl, J., Ryerson T.B., Science, vol. 351, issue 6279 (2016) pp. 1317–1320.
[9] Jacobson, G. A., Mater. Perform., vol. 46, issue 8 (2007) pp. 1-20.
[10] Venkatesan, R., Muthiah, M. A., Murugesh, P., Mar. Technol. Soc. J., vol. 48, issue 6 (2014) pp. 6–13.
[11] Chen, L., Wei, B., Xu, X., Coatings, vol. 11, issue 6. (2021) pp. 1-15.
[12] Zhang, L., Yu, X., L., Zhang, L., Yu, X., Zhang, Sun, H., Ge, Y., Wang, C.L., Limin, K., Jian Q., Huijuan G., ACS Omega, vol. 8, issue 15 (2023) pp. 13955–13966.
[13] Tripathi, A.K., Thakur, P., Saxena, P., Rauniyar, S., Gopalakrishnan, V., Front. Microbiol., vol. 12, issue 10 (2021) pp. 1–18.
[14] Marciales, A., Peralta, Y., Haile, T., Crosby, T., Wolodko, J., Corros. Sci., vol. 146, issue 7 (2019) pp. 99–111.
[15] Liu, H., Meng, G., Gu, T. W. L., Front. Microbiol., vol. 10, issue 6 (2019) pp. 1–13.
[16] Wu, T., Sun, C., Xu, J., Yan, M., Yin, F., Ke, W., Corros. Eng. Sci. Technol., vol. 53, issue 4 (2018) pp. 265–275.
[17] Zhang, G., Li, B., Liu, J., Luan, M., Yue, L., Jiang, X. T., Yu, K., Guan, Y., Microbiome, vol. 6, issue 1 (2018) pp. 222-234.
[18] Sadek, A., Chinthala, S.P., Senko, J. M., Monty, C. N. Corrosion, vol. 79, issue 8 (2023) pp. 957– 963.
[19] Lou, Y., Chang, W., Cui, T., Qian, H., Huang, L. Y., Ma, L., Hao, L., Hao, X., Zhang, D., Mater. Degrad., vol. 5, issue 1 (2021) pp. 59-75.
[20] Jamaluddin, N. A. A. Yusoff, M., Wee, S.K., Masri, M., Arch. Metall. Mater., vol. 67, issue 4 (2021) pp. 1355–1358.
[21] Videla, H. A., NACE - Int. Corros. Conf. Ser., vol. 96, issue 5 (1996) pp. 1-19.

[22] Zinkevich, V., Bogdarina, I., Kang, H., Hill, M. A. W., Tapper, R., Beech, I.B., Int. Biodeterior. Biodegrad., vol. 37, issue 4 (1996) pp. 163–172.
[23] Kappes, M. A., Corr. Rev., vol. 38, issue 1 (2020) pp. 1–24.
[24] Pessu, F., Barker, R., Neville, A., Corrosion, vol. 73, issue 9 (2017) pp. 1168–1183.
[25] Pessu, F., Hua, Y., Barker, R., Neville, A., Corrosion, vol. 74, issue 8 (2018) pp. 886–902.
[26] El Issmaeli, Y., Lahrichi, A., Kalanur, S.S., Natarajan, S.K., Pollet, B.G., Batteries, vol. 9, issue 5 (2023) pp. 1-26.
[27] Wei, J., Shen, W., Colloids Surfaces A Physicochem. Eng. Asp., vol. 643, issue 4 (2022) pp. 128754-12878.
[28] Schnaars, V., Wöhlbrand, L., Scheve, S., Hinrichs, C., Reinhardt, R., Rabus, R., Microb. Physiol., vol. 31, issue 1 (2021) pp. 36–56.
[29] Banker R. M. W., Coil, D. Frontiers in Marine Science, vol. 7, issue 7 (2020) pp. 1-18.
[30] Mahat, N. A. Othman, N. K. Sahrani, F. K., Idris, M. N., Sains Malaysiana, vol. 44, issue 11 (2015) pp. 1587–1591.
[31] Sharad A. A., Usup, G., Sahrani, F. K, Ahmad, A., AIP Conf. Proc., vol 1784, issue 1 (2016) pp. 20010-20026.
[32] Sharad A. A., Usup, G., Sahrani, F. K, Ahmad, A., Int. J. Adv. Sci. Tech. Res., vol. 6, issue 6, pp. 134–148.
[33] Al Abbas, F. M., Bhola, R., Spear, J. R., Olson, D. L., Mishra, B., Int. J. Electrochem. Sci., vol. 8, issue 1 (2013) pp. 859–871.
[34] Welikala, S., Al-Saadi, S., Gates, W. P., Panter, C., Singh Raman, R. K., Metals, vol. 12, issue 6 (2022) pp. 1-25.
[35] Potekhina, J. S. Sherisheva, N. G., Povetkina, L. P., Pospelove, A. P., Appl. Microbiol. Biotechnol., vol. 52, issue 5 (1999) pp. 639–646.
[36] Costa, O. Y. A., Raaijmakers, J. M., Kuramae, E. E., Frontiers in Microbiology, vol. 9, issue 5 (2018) pp. 1-25.
[37] Nielsen, K., Corros. J., vol. 22, issue 4 (1987) pp. 272–278.
[38] Tang, Y., Guo, X. P., Zhang, G. A., Corros. Sci., vol. 118, issue 7 (2017) pp. 118–128.
[39] J. X. J. Zhang, K. Hoshino, "Chapter 7 - Nanomaterials for molecular sensing," in Micro and Nano Technologies, J. X. J. Zhang and K. B. T.-M. S. and N. (Second E. Hoshino, Eds. Academic Press, (2019) pp. 413–487.
[40] Dong, Z. H., Shi, W., Ruan, H. M., Zhang, G. A., Corros. Sci., vol. 53, issue 9 (2011) pp. 2978–2987.
[41] Jefferson, K. K., FEMS Microbiol. Lett., vol. 236, issue 2 (2004) pp. 163–173.
[42] Dempsey, M. J., Mar. Biol., vol. 61, issue 4 (1981) pp. 305–315.
[43] Li, Y., Feng, S., Liu, H., Tian, X., Xia, Y., Li, M., Yu, H., Liu, Q., Chen, C., Corros. Sci., vol. 167, issue 5 (2020) pp. 108512-108530.
[44] Amendola, R., Acharjee, A. Frontiers in Microbiology, vol. 13, issue 4 (2022) pp. 1-23.
[45] Blackwood, D., Corros. Mater. Degrad., vol. 1, issue 1 (2018) pp. 59–76.
[46] Pal, M. K. Lavanya, M. J., Bio- Tribo-Corrosion, vol. 8, issue 3 (2022) pp. 76-92.
[47] Procópio, L., World J. Microbiol. Biotechnol., vol. 35, issue 5 (2019) pp. 73-90.
[48] Meyer, B., Int. Biodeterior. Biodegradation, vol. 51, issue 4 (2003) pp. 249–253.